Spectroscopic Evidence for Backbone Desolvation of Helical Peptides by 2,2,2-Trifluoroethanol: An Isotope-Edited FTIR Study†

Agnieszka Starzyk, Wendy Barber-Armstrong, Mohini Sridharan, and Sean M. Decatur*

Department of Chemistry, Carr Laboratory, Mount Holyoke College, South Hadley, Massachusetts 01075

Received August 27, 2004; Revised Manuscript Received October 18, 2004

ABSTRACT: 2,2,2-Trifluoroethanol (TFE) is widely used to induce helix formation in peptides and proteins, but the mechanism behind this effect is still poorly understood. Several recent papers have proposed that TFE acts by selectively desolvating the peptide backbone groups of the helix state. Infrared (IR) spectroscopy of the amide I band of polypeptides can be used to probe both secondary structure and backbone solvation, making this technique well suited for addressing the effect of TFE on polypeptide conformation. In this paper, we report the IR spectra as a function of TFE concentration for an alanine-rich peptide based on the repeat $(AAKAA)_n$. The IR spectra confirm that TFE desolvates the helical state of the peptide to a greater extent than the random coil state. Moreover, using a series of specifically ^{13}C-labeled peptides, the precise residues desolvated in the presence of TFE were identified. The residues most desolvated by TFE are the alanines located at position $i - 4$ in the sequence, where i is a lysine residue. This pattern of desolvation is consistent with molecular dynamics simulations which predict strong interactions between the lysine side chain at position n and the backbone carbonyl of the alanine at position $i - 4$. This is the first direct spectroscopic evidence of specific desolvation of helix backbone atoms in model alanine-rich peptides.

As first observed over 40 years ago, the addition of fluorinated alcohols [such as 2,2,2-trifluoroethanol (TFE)[1]] as cosolvents to aqueous solutions of peptides results in the induction or stabilization of the α-helix conformation (*1*). This "TFE effect" has been extensively applied to the study of structure and conformation in model peptides and protein fragments (*2*). Since most short peptides form marginally stable secondary structures in aqueous solutions, the addition of TFE to the solution is often necessary to enable the study of stable conformations outside the context of proteins.

Despite the widespread use of TFE as a helix-stabilizing agent, the mechanism of its action is still widely debated. While mechanisms in which TFE binds to residues in the helical conformation and stabilizes the structure have been proposed, there is no evidence for specific, direct interactions between TFE and hydrophobic side chains (*3*). However, recent molecular dynamics simulations (*4*) and NMR studies (*5*, *6*) suggest that TFE molecules may preferentially cluster around peptides in solution, reducing the hydration sphere around the peptide backbone. Several groups have proposed that helix induction can be explained by the effect of TFE on the structure of water and its solvation of peptide groups. On the basis of studies of highly helical alanine-rich peptides and a small organic model compound, Luo and Baldwin have proposed that desolvation of the backbone groups in the helical conformation strengthens intrahelical hydrogen bonding, thereby stabilizing the helix (*7*). In studies of coiled-coil peptides, Kentsis and Sosnick have proposed that the increased structure of TFE/water solutions desolvates peptide backbone groups in the unfolded state; this indirectly enhances the stability of the helical state (*8*). In a similar proposal, Cammers-Goodwin and co-workers point to the impact of helix hydration on the entropy of the system as the key to understanding the induction effect (*9*). In pure water, there is a greater ordering of the solvent shell around the helix compared to the random coil conformation, resulting in an unfavorable entropic change upon helix formation. By disrupting hydrogen bonding between the helical peptide backbone and solvent, TFE reduces the solvent ordering which occurs upon helix formation, stabilizing the helix relative to the coil state (*9*).

Beyond the TFE effect, several theoretical and experimental studies have identified solvent−backbone hydrogen bonding as an important (if not determining) factor behind the stability of α-helices formed by model alanine-rich peptides. Peptides based on alanine−lysine or alanine−arginine repeat sequences such as $(AAKAA)_n$ form stable, water-soluble α-helices and have become canonical model systems for probing helix properties, including the kinetics of helix formation (*10*−*12*), relative helix propensities of amino acids (*13*), and the helix dipole moment (*14*). However, there is debate in the literature on whether these peptides form truly "typical" helices or instead have unique physical properties due to the pattern of repeating charged groups. For example, helix propensities measured in these

† Supported by grants from the NSF (CHE9984844) and NIH (R15GM54334), a Henry Dreyfus Teacher Scholar Award (to S.M.D.), and a Howard Hughes Medical Institute Undergraduate Fellowship (to M.S.).

* To whom correspondence should be addressed. Fax: 413-538-2327. Telephone: 413-538-2115. E-mail: sdecatur@mtholyoke.edu.

[1] Abbreviations: TFE, 2,2,2-trifluoroethanol; IR, infrared; NMR, nuclear magnetic resonance; FTIR, Fourier transform infrared; HPLC, high-performance liquid chromatography; TFA, trifluoroacetic acid; CD, circular dichroism.

10.1021/bi0481444 CCC: $30.25
Published on Web 12/03/2004

peptides differ from those measured in proteins and other peptide systems (*15*, *16*), and this deviation might be due to differences in backbone−solvent hydrogen bonding. In molecular dynamics simulations of alanine-based helical peptides, Garcia and co-workers (*17*, *18*) and Vila et al. (*19*) have observed that lysine or arginine side chains partially shield backbone carbonyl groups; an arginine at position *i* in the helix shields a backbone carbonyl oxygen at position $i - 4$, resulting in a stronger hydrogen bond between the $i - 4$ carbonyl and the *i* amino group and a pronounced increase in helix propensity for the residue between at position $i - 2$ (*17*). Thus, charged amino acids with long side chains (such as arginine and lysine) may promote helix formation in alanine-rich peptides via selective partial desolvation of the helix backbone. While this model explains the unique helix propensity of alanine within these model peptides, there is no direct spectroscopic observation of site-specific desolvation of residues along the helix backbone.

Infrared (IR) spectroscopy of peptides and proteins, in particular of the amide I band, is commonly applied as a probe of secondary structure; α-helix, *β*-sheet, and random coil can be distinguished by characteristic amide I band frequency, line widths, and intensities (*20*, *21*). While the dependence of the amide I frequency on secondary structure is commonly exploited in experimental studies, the solvent sensitivity of the spectrum can also be used to probe protein structural features (*22*−*26*). The effect of hydrogen bonding and solvent polarity on the amide I band of model peptides, such as *N*-methylacetamide, has been well documented. In these compounds, hydrogen bonding causes a red shift in the amide I frequency (*22*−*24*). In polypeptides, the amide I band is similarly affected by solvent. The amide I frequencies for short helical peptides which are fully solvated in aqueous solution are lower than those reported for globular and membrane helical proteins; this difference can be attributed to the effect of water−peptide hydrogen bonding (*10*). DeGrado, Vanderkooi, and co-workers have used specific isotope labeling to distinguish between the amide I bands of interior and solvent-exposed residues in coiled-coil and helix bundle model peptides (*25*−*26*); these studies confirm that water−backbone hydrogen bonding results in a shift in the helical amide I band to lower frequency. The relationship between solvent−peptide hydrogen bonding, peptide conformation, and infrared spectroscopy has been explored in detail in a recent computational study, which predicts that site-specific backbone desolvation due to side chain shielding should be detectable using IR spectroscopy (*27*). The ability to probe both the conformation of the peptide backbone and the solvent−peptide hydrogen bonding via IR spectroscopy provides a window for directly observing the effect of TFE on solvent−peptide interactions in both α-helix and random coil states.

IR spectra of alanine-rich helical peptides in D_2O solution[2] have been reported by several groups (*28*−*36*); at low temperatures, when the peptides are primarily α-helical, the amide I′ mode occurs at ∼1633 cm^{-1}, while at high temperatures (when the peptide is primarily random coil) the band shifts to ∼1645 cm^{-1}. In this study, we use IR spectroscopy to probe the effect of TFE on helix stability and backbone solvation in an alanine-rich helical peptide. By measuring the IR spectra as a function of the percent of TFE at low temperature, we can assess the effect of TFE on the backbone solvation of the peptide in a helical conformation, while studies at higher temperatures give information on the hydration of the random coil conformation. When site-specific ^{13}C probes are introduced into the peptide backbone, the resulting isotope-shifted ^{13}C amide I′ band serves as a residue-specific probe for peptide conformation (*31*−*36*). This "isotope-edited" IR method has been used to assess the effect of capping groups (*32*) and side chains (*34*) on the backbone conformation of specific residues in the sequence of alanine-rich helical peptides. With the introduction of specific isotope labels, we can further observe the effect of TFE on the conformation and solvation of individual residues within the helix. Overall, we conclude that TFE enhances the dehydration of specific residues within the helix, and this enhancement is responsible for the increase in helix stability in TFE.

Table 1: Sequences of Peptides Used in This Study[a]

name	sequence
4Ac	Ac-AAAAKAAAAKAAAAKAAAAY-NH_2
4Anc	AAAAKAAAAKAAAAKAAAAY-NH_2
6mer	Ac-AAKAAY-NH_2
4AL1c	Ac-<u>AAAA</u>KAAAAKAAAAKAAAAY-NH_2
4AL2c	Ac-<u>AAAA</u>K<u>AAAA</u>KAAAAKAAAAY-NH_2
4AL3c	Ac-AAAAK<u>AAAA</u>K<u>AAAA</u>KAAAAY-NH_2
4AL4c	Ac-AAAAKAAAAK<u>AAAA</u>K<u>AAAA</u>Y-NH_2
4AL1nc	<u>AAAA</u>KAAAAKAAAAKAA<u>AAY</u>-NH_2
4AL2nc	<u>AAAA</u>K<u>AAAA</u>KAAAAKAAAAY-NH_2
4AL3nc	AAAAK<u>AAAA</u>K<u>AAAA</u>KAAAAY-NH_2
4AL4nc	AAAAKAAAAK<u>AAAA</u>K<u>AAAA</u>Y-NH_2
2LT	Ac-AAAAKA<u>AA</u>AKAAA<u>AKAA</u>AAY-NH_2
2LS	Ac-AAAAK<u>AAA</u>KAAAAKAAAAY-NH_2
1LN	Ac-AAAAK<u>A</u>AAA<u>A</u>KAAAAKAAAAY-NH_2
1LC	Ac-AAAAK<u>A</u>AAA<u>A</u>KAAAAKAAAAY-NH_2

[a] Underlined residues indicate positions of ^{13}C labels.

MATERIALS AND METHODS

Peptide Synthesis. Ten 25-residue peptides based on the $(AAKAA)_n$ repeat were synthesized, each differing in the number and position of ^{13}C-labeled residues (Table 1). All peptides were synthesized on a Pioneer automated peptide synthesizer (Applied Biosystems, Foster City, CA) using Fmoc chemistry. ^{13}C-Labeled peptides were synthesized by addition of *N*-Fmoc[1-^{13}C]alanine (Cambridge Isotope Laboratories) at the designated position in the sequence. Peptides were purified using reverse-phase HPLC. The masses of purified peptides were determined by electrospray mass spectrometry, and all were found to be in agreement with the expected values.

FTIR Sample Preparation. To remove residual trifluoroacetic acid (TFA) from the peptides as well as exchange amide N−H to N−D, about 2 mg of peptide was dissolved in 1−2 mL of 0.1% phosphoric acid/D_2O solution. This mixture was frozen and lyophilized to dryness. Lyophilized samples were then dissolved in 100 μL of D_2O or 100 mL of a mixture of D_2O and deuterated TFE (Cambridge Isotope Laboratories). The concentration of the peptide was measured via the ultraviolet absorbance of the tyrosine residue (at 274 nm, $\epsilon = 1450\ M^{-1}\ cm^{-1}$).

[2] D_2O is used instead of H_2O in IR studies in order to minimize the background absorbance of water. However, in D_2O the backbone amide proton is replaced with a deuteron, which results in an ∼10 cm^{-1} shift in the amide I band; this shifted band is referred to as amide I′.

FTIR Spectra. Samples were loaded into a water-jacketed, heatable solution cell with CaF_2 windows (Wilmad) and a 50 μm Teflon spacer. The water jacket of the cell was connected to a refrigerated circulating water bath (Neslab) used to control the sample temperature. Spectra were measured on a Bruker Equinox 55/S FTIR spectrometer, with the sample compartment purged continuously with dry N_2. Samples were equilibrated at the desired temperature for 10 min before measurement of spectra. Typically, 512 scans were collected and averaged at each temperature at a resolution of 4 cm^{-1}. Spectra of D_2O were also measured at each temperature and subtracted from the peptide spectra. All data analysis was performed using GRAMS/32 (Galactic Software).

Circular Dichroism Spectra. CD spectra of the peptides were collected from 280 to 185 nm wavelength range every 5 deg with a 100 ms time constant using an Aviv 215 CD spectrometer, equipped with a Peltier temperature-controlled cell jacket. Samples were equilibrated for 10 min at each temperature before scans were collected. The dynode voltage was maintained below 500 V throughout the measurements. Concentrations of the peptide solutions used to measure CD ($\sim$0.06 mM per peptide) were calculated as described for IR samples. The spectra were converted to molar ellipticity units after subtraction of baseline of just water measured at 25 °C (since there is no baseline fluctuation observed with change in temperature).

RESULTS

Circular Dichroism Spectra of 4Ac and 4Anc. At low temperatures in D_2O, 4Ac has a spectral signature characteristic of an α-helix, with negative features at 222 and 208 nm; as the temperature increases, the spectrum changes to that of a random coil. The 4Anc peptide is much less structured at low temperatures, but also its random coil content increases as the temperature increases. Melting curves ($[\theta]_{222}$ vs temperature) are given in Figure 1. As the percent TFE increases, the $[\theta]_{222}$ of 4Anc at 0 °C decreases substantially and at 40% TFE is close to that of the 4Ac peptide (Figure 1A). Increasing TFE makes the melting curves of each peptide less cooperative, and at 40% TFE there appears to be a significant amount of helix present in both peptides at temperatures as high as 85 °C.

IR Spectra of 4Ac and 4Anc. FTIR spectra of 4Ac and 4Anc in D_2O and 40% TFE are shown in Figure 2. The amide I′ of the 4Ac peptide at 0 °C shifts 5 cm^{-1} from 1633 to 1638 cm^{-1} upon going from D_2O to 40% TFE, while the amide I′ frequency of 4Anc is unchanged. For both peptides, the spectra in 40% TFE are broader and with a lower maximum absorbance than the D_2O spectra. For the 4Ac peptide in D_2O, the amide I′ band decreases in intensity and shifts to higher frequency as the temperature increases; these changes are consistent with previously observed spectra (*31*−*34*). In 40% TFE, there are also spectral changes with temperature (a shift to higher frequency and a decrease in intensity), but much smaller than in D_2O.

IR Spectra of the 6mer Peptide. To observe the effect of TFE on the conformation and spectra of a nonhelical peptide, a short 6mer, Ac-AAKAAY-NH_2, was prepared. The IR spectra of this peptide in water and 40% TFE are shown in Figure 3. In the IR spectra, the amide I′ bands in both D_2O and 40% TFE have maxima at $\sim$1650 cm^{-1}, though the D_2O spectrum is significantly broader than the 40% TFE spectrum (Figure 3B). In both water and 40% TFE, the CD spectra of the 6mer suggest that the conformation is primarily random coil (data not shown).

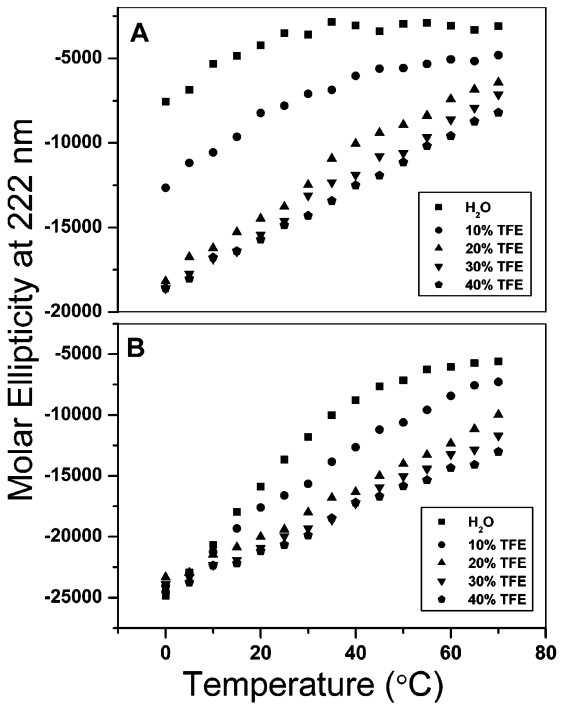

FIGURE 1: CD melting curves for 4A peptides uncapped (A) and capped (B) in varying percent TFE solutions.

IR Spectra of Labeled Peptides. The IR spectra of the capped labeled peptides at 0 °C in D_2O and 40% TFE are shown in Figure 4. In the D_2O spectra, a prominent ^{13}C amide I′ band is well resolved in 4AL1c, 4AL2c, and 4AL3c at $\sim$1598 cm^{-1}, while 4AL4c has a poorly resolved ^{13}C amide I′ band. This is consistent with the presence of a stabilized helix at the N-terminus and central regions of the peptide, while the C-terminus is frayed (*30*, *31*). In 40% TFE, however, there are two ^{13}C amide I′ bands clearly resolved in the 4AL2c and 4AL3c spectra, one at $\sim$1598 cm^{-1} and the other at $\sim$1620 cm^{-1}. There is also evidence for an additional ^{13}C band at $\sim$1619 cm^{-1} in the second derivative of the 4AL1c spectrum, though it is poorly resolved in the absorption spectrum. A similar trend is seen in the uncapped peptides (Figure 5); in 40% TFE, 4AL2nc and 4AL3nc have two ^{13}C amide I′ bands at $\sim$1598 and $\sim$1619 cm^{-1}, although the feature is poorly resolved. At 65 °C, the spectra of 4AL2c, 4AL2nc, 4AL3c, and 4AL3nc in 40% TFE still have prominent features at $\sim$1620 and $\sim$1598 cm^{-1} (Figure 6).

IR Spectra of Doubly and Singly Labeled Peptides. To assign the ^{13}C spectral transition at higher resolution, a set of doubly and singly labeled peptides, 2LS, 2LT, 1LN, and 1LC, were prepared. IR spectra of these peptides in D_2O and 40% TFE are shown in Figure 7. For both peptides in D_2O, a single ^{13}C amide I′ band is present. The ^{13}C amide I′ for 2LS is shifted to lower frequency than that of 2LT due to the dependence of the coupling on the distance and relative geometry of the ^{13}C labels (*34*, *35*). In TFE, both the ^{12}C and ^{13}C amide I′ bands broaden and shift to higher frequency; a new feature, however, appears in the ^{13}C amide I′ region

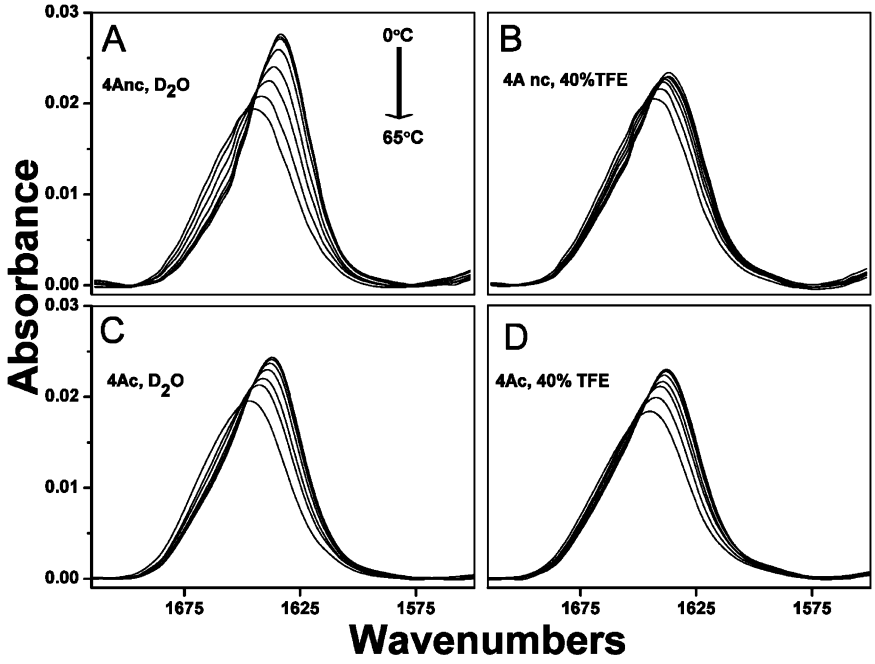

FIGURE 2: FTIR spectra of the amide I′ band region of 4A peptides in D_2O and 40% D_2O/TFE solutions. Spectra were measured at 0, 5, 15, 25, 35, 45, 55, and 65 °C.

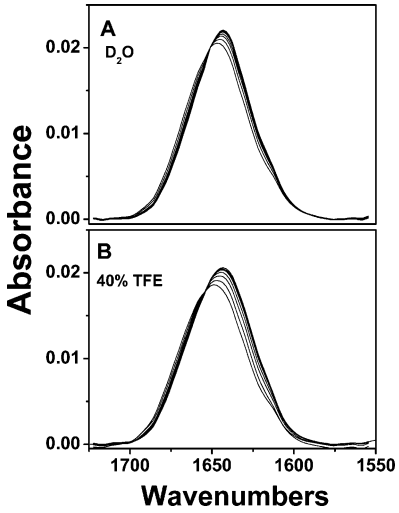

FIGURE 3: FTIR spectra of amide I′ bands of the 6mer peptide in (A) D_2O and (B) 40% TFE/D_2O solution. Spectra were measured at 0, 5, 15, 25, 35, 45, 55, and 65 °C.

of the 2LS peptide, at ~1619 cm^{-1} (Figure 7B); this band is more clearly visible in the second derivative spectra (Figure 7F).

Differences between the alanine at the N-terminal side of this central block of four alanines and the alanine at the C-terminal side can be seen in the spectra for 1LN and 1LC (Figure 7C,D). In D_2O, both 1LN and 1LC give a single ^{13}C amide I′ band; the band for 1LC is shifted slightly to lower frequency than that of 1LN (Figure 7C,D). When these peptides are placed in 40% TFE, the 1LN peptide shows an additional feature at 1619 cm^{-1}, even more prominent in the second derivative spectrum (Figure 7G,H).

DISCUSSION

TFE Reduces Helix Backbone−Solvent Hydrogen Bonding. According to the CD spectra, the addition of TFE results in an increase in helix content for the 4A peptides, as well as in an increase in helix stability upon thermal melting. In the IR spectra of the peptides, the amide I′ bands of 4Ac and 4Anc are shifted to higher frequency in 40% TFE compared to D_2O. Because the helix content is increasing upon transfer from D_2O to 40% TFE, the shift to higher frequency is due to a reduction in solvent−backbone hydrogen bonding for the helix; this shift is consistent with desolvation effects observed in other systems (*25*, *26*) and predicted in simulations (*27*). In addition to shifting to higher frequency, the amide I′ band also broadens and decreases in intensity at the maximum. This is likely due to the presence of both some hydrogen-bonded and dehydrated carbonyls along the helix, giving rise to a heterogeneously broadened amide I′ band. Thus, the IR spectra of 4Ac and 4Anc indicate that the addition of TFE to solution partially desolvates the backbone carbonyl groups of the α-helix.

Short peptides, such as the 6mer used in this study, are often used as models for the "random coil" state of longer polypeptides (*7*).[3] According to CD spectra, the short 6mer peptide is not helical in D_2O or 40% TFE (data not shown). Furthermore, in the IR spectra, the amide I′ frequency of the short 6mer peptide does not change upon addition of TFE (Figure 3). Since this peptide shows no evidence of an amide I′ band shift associated with a reduction in backbone−solvent hydrogen bonding, we conclude that a nonhelical polypeptide (such as the 6mer) is not desolvated by TFE to the same extent as a helical peptide: in other words, *TFE reduces solvent−backbone hydrogen bonding to helical residues but not random coil residues.* These observations are consistent with molecular dynamics simulations which indicate stronger interactions between TFE and α-helical residues compared to other backbone conformations (*4*).

[3] Recent studies demonstrate that short peptides such as a trimer may partially adopt polyproline II conformations (*37*, *38*), and evidence for the polyproline II conformation has also been observed in the unfolded state of a number of proteins (*39*), raising the possibility that the peptides exhibiting CD spectra indicative of random coil may adopt ordered structures. See ref *40* for more details.

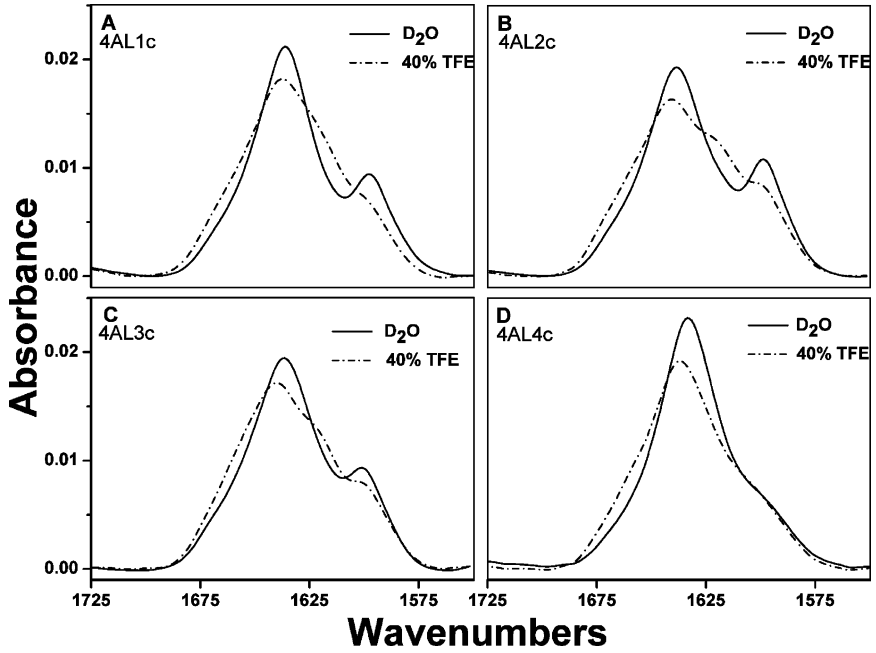

FIGURE 4: Amide I′ bands of labeled 4A capped peptides in D_2O (solid lines) and 40% TFE/D_2O solution (dashed lines). Spectra were recorded at 0 °C. (A) 4AL1 capped. (B) 4AL2 capped. (C) 4AL3 capped. (D) 4AL4 capped.

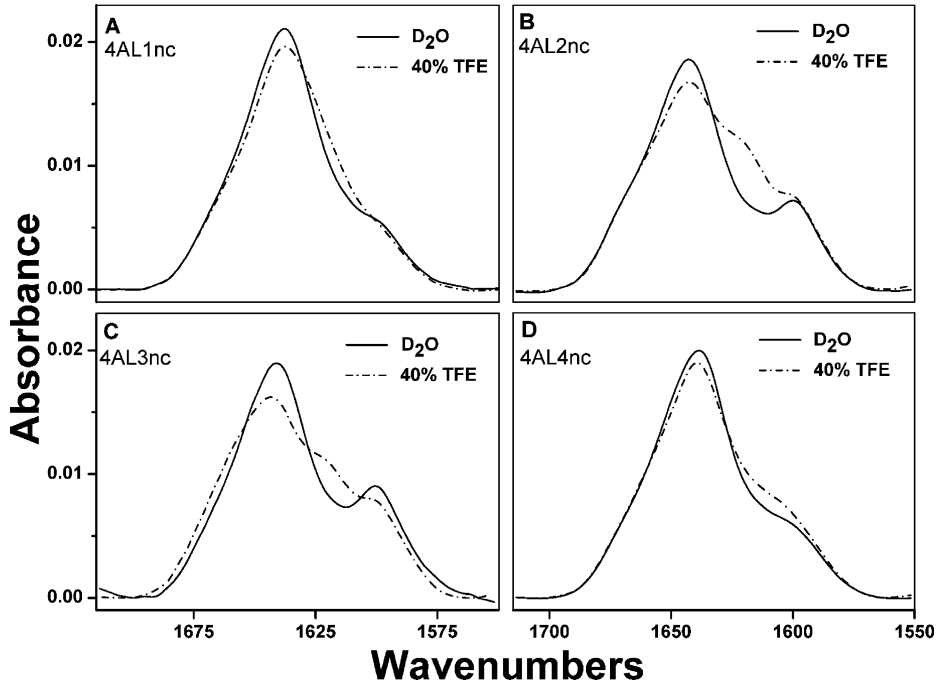

FIGURE 5: Amide I′ bands of labeled 4A uncapped peptides in D_2O (solid lines) and 40% TFE/D_2O solution (dashed lines). Spectra were recorded at 0 °C. (A) 4AL1 uncapped. (B) 4AL2 uncapped. (C) 4AL3 uncapped. (D) 4AL4 uncapped.

Stronger interactions between TFE and the helix reduce the number of water molecules around the helix backbone and therefore reduce backbone−water hydrogen bonding.

The observed amide I′ band shift to higher frequency for 4A is consistent with a reduction in the solvent−helix backbone hydrogen bonding upon addition of TFE. As an aside, these results illustrate the need for caution when interpreting amide I′ band shifts in terms of conformational changes: in thermal melting studies in D_2O solution, a shift to higher frequency for helical peptides is generally indicative of helix unfolding, yet in this study, the amide I′ band shift to higher frequency in 40% TFE correlates with an *increase* in helix content. These results demonstrate that care must be taken in interpreting infrared spectra to distinguish between effects of conformation and effects of solvation in protein folding studies.

Effects of TFE on Conformation and Stability of N-Terminal Residues. Interestingly, the 4Ac and 4Anc peptides have nearly identical CD spectra in 40% TFE, suggesting that in 40% TFE the presence or absence of the capping group does not impact the conformation and relative stability of the helix; this is quite different than previously observed results in D_2O (*31*). The IR spectra of 4AL1c and 4AL1nc also look similar in 40% TFE, while they are quite different in D_2O (Figures 4A and 5A). This suggests that the first

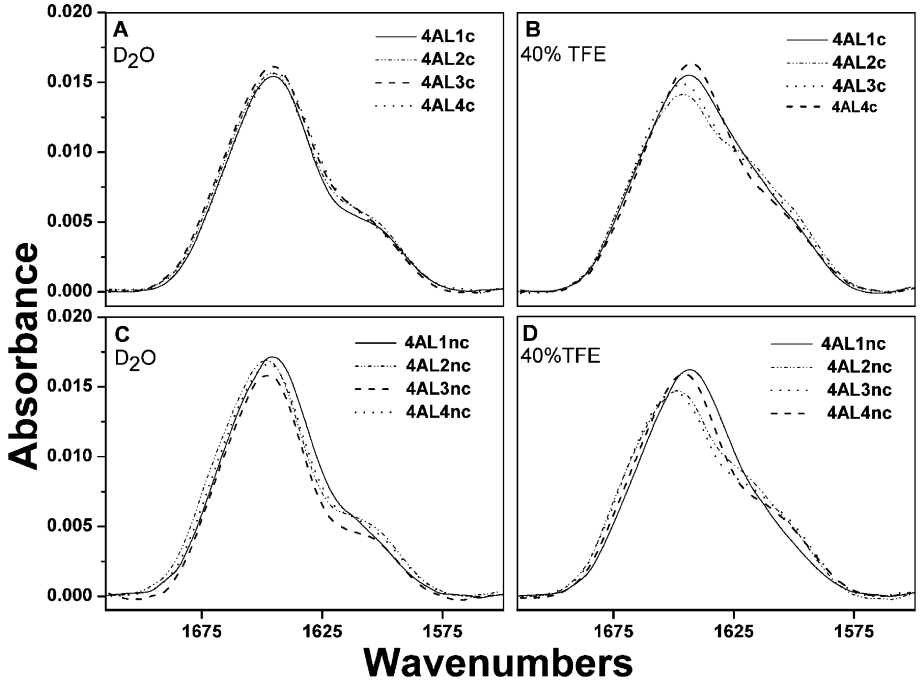

FIGURE 6: Amide I′ band spectra of labeled capped and uncapped 4A peptides at 65 °C in D_2O and 40% TFE/D_2O solution. (A) Labeled capped peptides in D_2O at 65 °C. (B) Labeled uncapped peptides in 40% TFE/D_2O at 65 °C. (C) Labeled uncapped peptides in D_2O at 65 °C. (D) Labeled uncapped peptides in 40% TFE/D_2O solution.

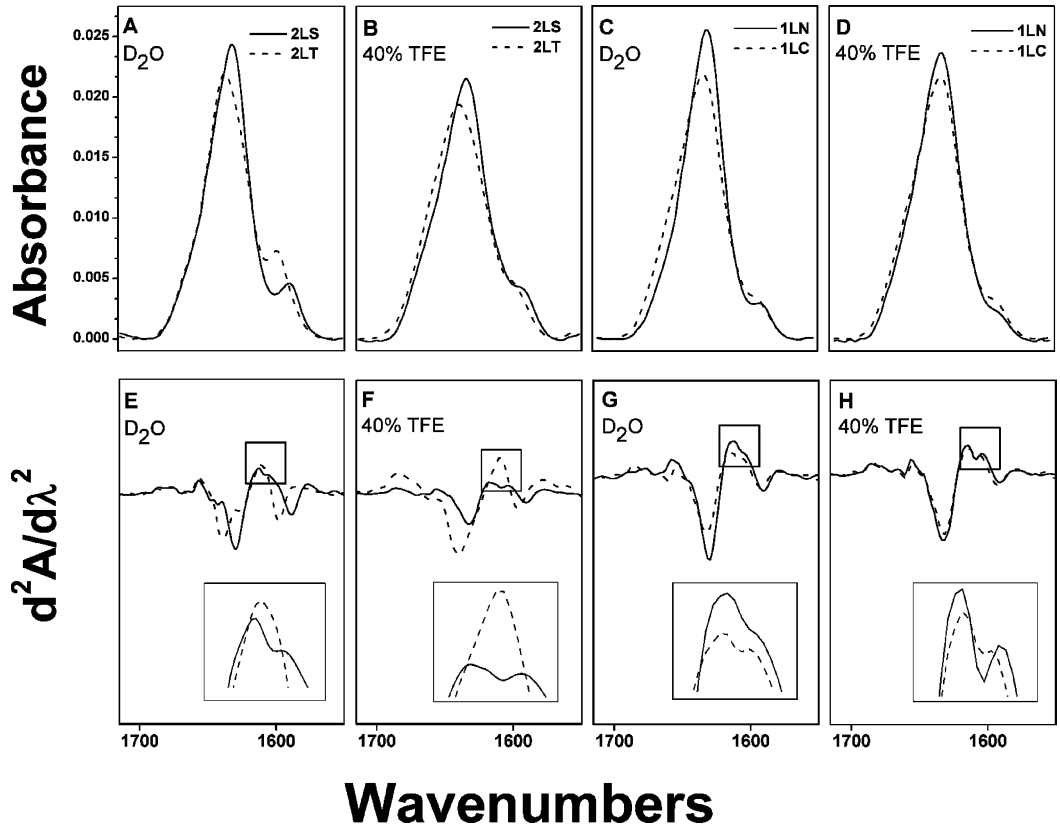

FIGURE 7: Amide I′ band spectra of 2LS, 2LT, 1LN, and 1LC in D_2O and 40% TFE/D_2O solution at 0 °C. (A−D) Amide I′ spectra measured in D_2O at 0 °C. (E−H) Second derivatives of the amide I′ spectra. Insets show expansions of the boxed portions of the spectra.

four alanines adopt similar conformations in both 4Ac and 4Anc when in 40% TFE.

The first four residues of the helix each form only one intrahelical hydrogen bond with their carbonyls paired to the NH groups $i + 4$ in the sequence. The NH groups of these residues do not form intrahelical hydrogen bonds but rather are free to interact with solvent or capping groups. In some peptides, this results in "fraying" of the N-terminus, with the residues forming more favorable hydrogen bonds with water rather than within the helix (*32*). The reduction in the number of water molecules surrounding the peptide may also reduce the possibility of these residues forming hydrogen

bonds with water, favoring the formation of intrahelical hydrogen bonds even in the absence of a capping group. Thus, at least part of the helix induction effect of TFE involves stabilizing the helix conformation among the N-terminal residues.

Backbone Dehydration Occurs at Specific Residues in the Sequence. The broadening of the amide I′ band of 4Ac in the presence of 40% TFE indicates that there are both hydrated and dehydrated populations of carbonyls present in solution. To determine the location and distribution of backbone dehydration sites within the helix sequence, the IR spectra of specifically ^{13}C-labeled peptides were measured in D_2O and 40% TFE. The presence of two ^{13}C amide I′ bands in the 40% TFE spectra of the 4AL2 and 4AL3 peptides is consistent with the presence of solvated (1598 cm^{-1}) and desolvated (1619 cm^{-1}) helical residues. In the doubly and singly labeled peptides, we can isolate this effect further to the residue which follows a lysine residue in the sequence; 1LN shows evidence of a split ^{13}C amide I′, with a 1619 cm^{-1} component which becomes significant at 40% TFE. There is a smaller 1619 cm^{-1} feature present in the spectrum of the 1LC peptide but none in the 2LT spectrum.

Dehydration of the residue directly adjacent to the lysine in these alanine−lysine repeat peptides is consistent with molecular dynamics simulations by Garcia et al., in which an arginine residue at position *i* interacts with the backbone carbonyl at position $i - 4$ (*17*, *18*). This is the position of the labeled residue in the 1LN peptide:

…… K **A** A A A K …….

i-5 i-4 i-3 i-2 i-1 i

The split ^{13}C amide I′ band in the spectrum of 1LN in 40% TFE suggests that the $i - 4$ residue spends a significant amount of time both desolvated (1619 cm^{-1}) and solvated (1598 cm^{-1}). While the molecular dynamics simulations of Garcia et al. were performed in water, not a water/TFE mixture, it may be that the TFE effect amplifies the specific dehydration of the $i - 4$ alanine, making it clearer to detect spectroscopically. These results are in excellent agreement with a recently published simulation of hydration of the 4Ac peptide, in which the carbonyl labeled in 1LN is more shielded from hydrogen bonding than the carbonyl in 1LC (*27*). This is the first example of direct spectroscopic evidence of side chain−backbone interactions in alanine-rich peptides, and these observations indicate that isotope-edited IR spectra may be a well-suited technique to dissect these interactions.

Conclusions. IR spectra of alanine-rich peptides support a model of helix induction by TFE involving disruption of hydrogen bonding between the solvent and the helix backbone. As indicated by the IR spectra of the amide I′ band, TFE dehydrates backbone atoms in the helix conformation but not in the random coil conformation. By reducing the number of helix backbone−solvent hydrogen bonds, the addition of TFE may lower the entropy cost of forming a helix by reducing the amount of solvent ordering which occurs upon helix formation. Isotope-edited IR spectra indicate that the most dehydrated carbonyl belongs to the alanine residues which are $i - 4$ in the sequence from lysine residues, suggesting direct interactions between lysine side chains and helix backbone atoms; these interactions may also play a role in helix stabilization.

ACKNOWLEDGMENT

Mass spectra were measured at the University of Massachusetts mass spectrometry facility; we thank Dr. Steven Eyles for assistance.

REFERENCES

1. Goodman, M., and Listowsky, I. (1962) Conformational aspects of synthetic polypeptides. VI. Hypochromic spectral studies of oligo-γ-methyl-L-glutamate peptides, *J. Am. Chem. Soc. 84*, 3770−3771.
2. Buck, M. (1998) Trifluoroethanol and colleagues: Cosolvents come of age, *Q. Rev. Biophys. 31*, 297−355.
3. Storrs, R. W., Truckses, D., and Wemmer, D. E. (1992) Helix propagation in trifluoroethanol solutions, *Biopolymers 32*, 1695−1702.
4. Roccatano, D., Colombo, G., Fiorini, M., and Mark, A. E. (2002) The mechanism by which 2,2,2-trifluorethanol/water mixtures stabilize secondary structure formation in peptides: A molecular dynamics study, *Proc. Natl. Acad. Sci. U.S.A. 99*, 12179−12184.
5. Fiorini, M., Diaz, M. D., Burger, K., and Berger, S. (2002) Solvation phenomena of a tetrapeptide in water/trifluoroethanol and water/ethanol mixtures: Diffusion, intermolecular NOE and molecular dynamics study, *J. Am. Chem. Soc. 124*, 7737−7744.
6. Diaz, M. D., Fiorini, M., Burger, K., and Berger, S. (2002) Evidence of complete hydrophobic coating of bombesin by trifluoroethanol in aqueous solution: A NMR and molecular dynamics study, *Chem. Eur. J. 8*, 1663−1669.
7. Luo, P., and Baldwin, R. L. (1999) Interactions between water and polar groups of the helix backbone: An important determinant of helix propensities, *Proc. Natl. Acad. Sci. U.S.A. 96*, 4930−4935.
8. Kentsis, A., and Sosnick, T. R. (1998) Trifluoroethanol promotes helix formation by destabilizing backbone exposure: Desolvation rather than native hydrogen bonding defines the kinetic pathway of dimeric coiled-coil formation, *Biochemistry 37*, 14613−14622.
9. Walgers, R., Lee, T. C., and Cammers-Goodwin, A. (1998) An indirect chaotropic mechanism for the stabilization of helix conformation of peptides in aqueous trifluoroethanol and hexafluoro2-propanol, *J. Am. Chem. Soc. 120*, 5073−5079.
10. Williams, S., Causgrove, T. P., Gilmanshin, R., Fang, K. S., Callendar, R. H., Woodruff, W. H., and Dyer, R. B. (1996) Fast events in protein folding: Helix melting and formation in a small peptide, *Biochemistry 35*, 691−697.
11. Huang, C.-Y., Getahun, Z., Wang, T., DeGrado, W. F., and Gai, F. (2001) Temperature-dependent helix-coil transition of an alanine based peptide, *J. Am. Chem. Soc. 123*, 12111−12112.
12. Huang, C.-Y., Klmeke, J. W., Getahun, Z., DeGrado, W. F., and Gai, F. (2001) Time-resolved infrared study of the helix-coil transition using 13 C labeled helical peptides, *J. Am. Chem. Soc. 123*, 9325−9328.
13. Rohl, C. A., and Baldwin, R. L. (1998) Deciphering the rules of helix stability in peptides, *Methods Enzymol. 295*, 1−26.
14. Lockhart, D. J., and Kim, P. S. (1992) Internal stark effect measurement of the electric field at the amino terminus of an alpha helix, *Science 257*, 947−951.
15. Vila, J., Williams, R. L., Grant, J. A., Wojcik, J., and Scheraga, H. A. (1992) Intrinsic helix forming tendency of L-alanine, *Proc. Natl. Acad. Sci. U.S.A. 89*, 7821−7825.
16. Williams, L., Kather, K., and Kemp, D. S. (1998) High helicities of Lys-containing, Ala-rich peptides are primarily attributable to a large, context-dependent Lys stabilization, *J. Am. Chem. Soc. 120*, 11033−11043.
17. Garcia, A. E., and Sanbonmatsu, K. Y. (2002) α-Helical stbilization by side chain shielding of backbone hydrogen bonds, *Proc. Natl. Acad. Sci. U.S.A. 99*, 2782−2787.
18. Ghosh, T., Garde, S., and Garcia, A. E. (2003) Molecular evidence for alpha-helix stabilization by shielding of the backbone hydrogen bonds by side chains, *Biophys. J. 85*, 3187−3193.
19. Vila, J., Ripoll, D. R., and Scheraga, H. A. (2000) Physical reasons for the unusual α-helix stabilization afforded by charged or neutral polar residues in alanine-rich peptides, *Proc. Natl. Acad. Sci. U.S.A. 89*, 7821−7825.

20. Surewicz, W. K., Mantsch, H. H., and Chapman, D. (1993) Determination of protein secondary structure by Fourier transform infrared spectroscopy: A critical assessment, *Biochemistry 32*, 389−394.
21. Barth, A., and Zscherp, C. (2002) What vibrations tell us about proteins, *Q. Rev. Biophys. 35*, 369−430.
22. Gerothanassis, I. P., and Vakka, C. (1994) ^{17}O NMR chemical shifts as a tool to study specific hydration sites of amides and peptides: Correlation with the IR amide I stretching vibration, *J. Org. Chem. 59*, 2341−2348.
23. Gerothanassis, I. P., Birlirakis, N., Karayannis, T., Sakarellos-Daitsiotis, M., Sakarellos, C., Vitoux, B., and Marraud, M. (1992) Hydration of the Gly2 and Gly3 peptide oxygens of [Leu5]-enkephalin in aqueous solution as revealed by the combined use of ^{17}O-NMR and Fourier-transform infrared spectroscopy, *Eur. J. Biochem. 210*, 693−698.
24. Eaton, G., and Symons, M. C. R. (1988) Solvation spectra 80. Spectroscopic studies of the solvation of n,n-dimethyl amides in pure and mixed-solvents, *J. Chem. Soc., Faraday Trans. 1 84*, 3459.
25. Manas, E. S., Getahun, Z., Wright, W. W., DeGrado, W. F., and Vanderkooi, J. M. (2000) Infrared spectra of amide groups in a-helical proteins: Evidence for hydrogen bonding to water, *J. Am. Chem. Soc. 122*, 9883−9890.
26. Walsh, S. T. R., Cheng, R. P., Wright, W. W., Alonso, D. O. V., Daggett, V., Vanderkooi, J. M., and DeGrado, W. F. (2003) The hydration of amides in helices: a comprehensive picture from molecular dynamics, IR and NMR, *Protein Sci. 12*, 520−531.
27. Gnanakaran, S., Hochstrasser, R. M., and Garcia, A. E. (2004) Nature of structural inhomogeneities on folding a helix and their influence of spectral measurements, *Proc. Natl. Acad. Sci. U.S.A. 101*, 9229−9234.
28. Graff, D. K., Pastran-Rios, B., Venyaminov, S. Yu., and Prendergast, F. G. (1997) Fourier transform infrared spectroscopy and two-dimensional infrared analysis of model helical peptides, *J. Am. Chem. Soc. 119*, 11282−11294.
29. Yoder, G., Pancoska, P., and Keiderling, T. A. (1997) Characterization of alanine rich peptides of the general formula Ac-$(AAKAA)_n$-GY-NH_2 using vibrational circular dichroism and Fourier transform IR, *Biochemistry 36*, 15123−15133.
30. Martinez, G., and Millhauser, G. (1995) FTIR spectroscopy of alanine-based peptides: Assignment of the amide I′ modes for random coil and helix, *J. Struct. Biol. 114*, 23−37.
31. Decatur, S. M., and Antonic, J. (1999) Isotope-edited infrared spectroscopy of helical peptides, *J. Am. Chem. Soc. 121*, 11914−11915.
32. Decatur, S. M. (2000) Infrared spectroscopy of isotopically labeled helical peptides: Probing the effects on N-acetylation on helix stability, *Biopolymers 54*, 180−185.
33. Silva, R. A. G. D., Kubelka, J., Bour, P., Decatur, S. M., and Keiderling, T. A. (2000) Site-specific conformational determination in thermal unfolding studies of helical peptides using vibrational circular dichroism with isotopic substitution, *Proc. Natl. Acad. Sci. U.S.A. 97*, 8318−8323.
34. Silva, R. A. G. D., Nguyen, J. Y., and Decatur, S. M. (2002) Probing the effects of side chains on the conformation and stability of helical peptides via isotope-edited infrared spectroscopy, *Biochemistry 41*, 15296−15303.
35. Barber-Armstrong, W., Donaldson, T., Wijesooriya, H., Silva, R. A. G. D., and Decatur, S. M. (2004) Empirical relationships between isotope-edited IR spectra and helix geometry, *J. Am. Chem. Soc. 126*, 2356−2354.
36. Huang, R., Kubelka, J., Barber-Armstrong, W., Silva, R. A. G. D., Decatur, S. M., and Keiderling, T. A. (2004) The nature of vibrational coupling in helical peptides: An isotope-labeling study, *J. Am. Chem. Soc. 126*, 2339−2345.
37. Eker, F., Griebenow, K., Cao, X., Nafie, L. A., and Schweitzer-Stenner, R. (2004) Preferred peptide backbone conformations in the unfolded state revealed by the structure analysis of alanine-based (AXA) tripeptides in aqueous solution, *Proc. Natl. Acad. Sci. U.S.A. 101*, 10054−10059.
38. Eker, F., Cao, X., Nafie, L., and Schweitzer-Stenner, R. (2002) Tripeptides adopt stable structures in water. A combined polarized visible Raman, FTIR, and VCD spectroscopy study, *J. Am. Chem. Soc. 124*, 14330−14341.
39. Keiderling, T. A., and Xu, Q. (2002) Unfolded peptides and proteins studied with infrared absorption and vibrational circular dichroism spectra, *Adv. Protein Chem. 62*, 111−161.
40. Shi, Z., Woody, R. W., and Kallenbach, N. R. (2002) Is polyproline II a major backbone conformation in unfolded proteins?, *Adv. Protein Chem. 62*, 163−240.

BI0481444